Mesozoic–Cenozoic tectonothermal evolution of the eastern part of the Tibetan Plateau (Songpan-Garzê, Longmen Shan area): insights from thermochronological data and simple thermal modelling

FRANÇOISE ROGER[1]*, MARC JOLIVET[1,2], RODOLPHE CATTIN[1] & JACQUES MALAVIEILLE[1]

[1]*Université Montpellier 2, Laboratoire Géosciences Montpellier CNRS-UMR 5243, Place Eugène Bataillon, F-34095 Montpellier Cedex 05, France*

[2]*Université Rennes 1, Laboratoire Géosciences Rennes, CNRS-UMR 6118, Bat 15, Campus de Beaulieu, F-35042 Rennes Cédex, France*

**Corresponding author (e-mail: Francoise.Roger@gm.univ-montp2.fr)*

Abstract: We present a synthesis of the tectonic and thermochronological evolution of the Eastern Tibet since the Triassic. The long-term cooling histories obtained on magmatic and metamorphic rocks of the South Songpan-Garzê, Kunlun and Yidun blocks are similar showing a very slow and regular cooling during Late Jurassic and Cretaceous, confirming the suspected lack of major tectonic events between *c.* 150 and 30 Ma. The exhumation linked to the Tertiary growth of the Tibetan Plateau initiated around 30 Ma and concentrates at the vicinity of the major tectonic structures. Exhumation rates increased again from about 7 Ma in the Longmen Shan.

To interpret this very slow cooling rate between Late Jurassic and Early Cenozoic from granites of this area, we use a simple 1D thermal model that takes into account the thermal properties of both sediments and crust. The results suggest that: (1) high temperature (500 °C) can be kept over a long period of time; (2) during Cretaceous, cooling is mostly controlled by the thermal properties of sediments of continental origin; and (3) the initial Late Triassic rapid cooling rate was caused by the large thermal contrast between the granite body and the sedimentary rocks rather than by a high exhumation rate.

The tectonic evolution of northeastern Tibet presents intriguing features. First in this area, most of the rocks presently exposed consist of flyschoid Triassic sequences showing widespread deformations (the series are deformed into a wide accretionary fold–thrust belt) and very low metamorphism. This suggests that since the Triassic orogeny, this area has only been submitted to very low erosion and exhumation rates. Furthermore despite the huge distances that separate the sampled locations, the studies of South Songpan-Garzê, Kunlun, and Yidun granites suggest a homogeneous thermal evolution for the whole North-Eastern Tibet. All these granite plutons exhibit a similar three stages thermal evolution, which includes: (1) a short period (<10 Ma) of rapid cooling after their emplacement during late Triassic; (2) a long period (at least 100 Ma) of thermal stability; and (3) a final Middle Tertiary exhumation. No satisfying explanation has yet been proposed to explain this original behaviour.

Here using a synthesis of structural and thermochronological data combined with a simple modelling of the tectono-thermal behaviour of the lithosphere, we discuss the relative effect of first-order parameters that played a great part in this evolution from Triassic to present.

The Triassic fold belt of NE Tibet results from interactions between the south China, north China and Qiangtang (north Tibet) blocks during the Indosinian orogeny (e.g. Pullen *et al.* 2008; Roger *et al.* 2008). It is mainly composed, from west to east, of the Bayan Har, Songpan-Garzê, and Yidun (or Litang-Batang) terranes (Fig. 1).

In Permian times, due to the opening of the Neotethys, the Qiangtang block, which was part of the Cimmerian continent detached from the Gondwanan continent, migrated northwards, closing the Palaeotethys (Fig. 2a). A synchronous activity along three subduction zones, Kunlun-Anyemaqen to the north, Jinsha to the south and Yushu-Batang to the east, induced the growth of a wide accretionary orogen until the end of the Triassic period. The Songpan ocean formed the eastern domain of the Palaeotethys and was divided into two main basins (Roger *et al.* 2008). The first one developed towards the east due to differential motion between the north China Block and the south China Block

From: Gloaguen, R. & Ratschbacher, L. (eds) *Growth and Collapse of the Tibetan Plateau.* Geological Society, London, Special Publications, **353**, 9–25.
DOI: 10.1144/SP353.2 0305-8719/11/$15.00

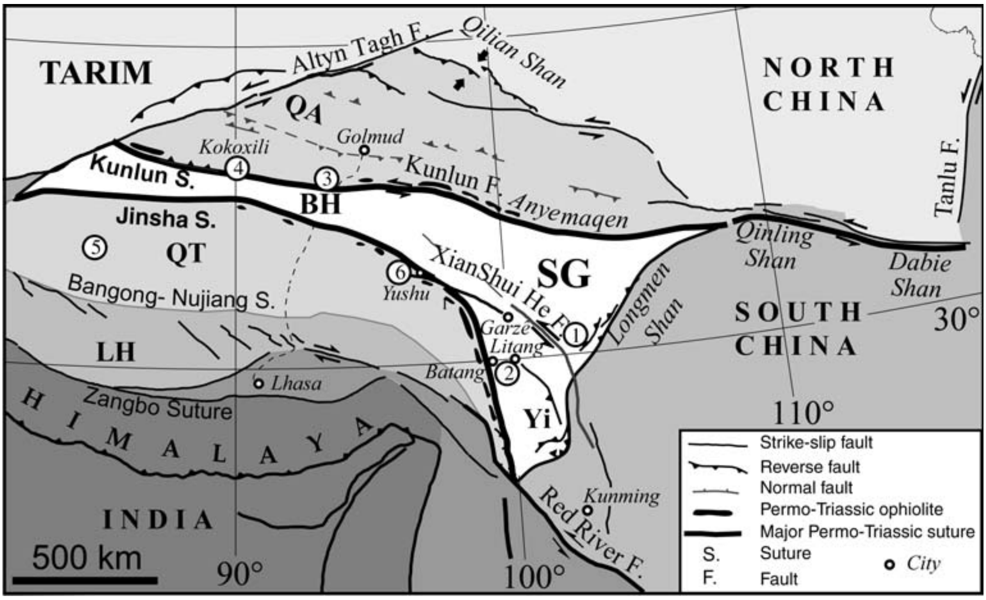

Fig. 1. Geographical extension of the Songpan-Garzê belt. The white area represents the current extension of the Triassic belt (after Roger *et al.* 2008). SG, Songpan-Garzê belt; BH, Bayan Har terrane; Yi, Yidun (or Litang-Batang) block;LH, Lhasa block; QT, Qiangtang block; QA, Kunlun-Qaidam block.1, rocks of the South Songpan-Garzê area; 2, granites of Yidun block; 3, Xidatan gneiss; 4, Kokoxili granites; 5, blueschist of Gangma Co; 6, granites of Yushu. Numbers (1, 2, 3, 4) refer to cooling histories presented from Figures 5 and 6.

(Songpan-Garzê basin) (Zhang *et al.* 2006). The second basin (Garzê-Litang or Yidun basin) was a marginal basin developed in a back-arc setting, following the Permian rifting event (Panxi Rift), which separated the Yidun block from the south China–Indochina Craton (e.g. Roger *et al.* 2008, 2010; Zi *et al.* 2008). The east dipping subduction zone (Yushu-Batang) that generated the Yidun calc-alkaline granites (245–229 Ma) was thus located west of the Yidun block (Reid *et al.* 2007). This subduction, together with the Jinsha subduction zone further west, accommodated the closure of the wide Palaeotethys ocean. To the northwest, the Yushu-Batang subduction became intra-oceanic and joined the Kunlun-Anyemaqen subduction zone to the north. The subsequent arc-type volcanism formed the intra-oceanic Yushu arc (Fig. 2b).

Along the northern and western border of the south China block, the Songpan-Garzê and Litang basins were limited by a passive margin (Mattauer *et al.* 1992; Calassou *et al.* 1994; Roger *et al.* 2004; Zhang *et al.* 2006). The sedimentation in the oceanic basins was characterized by thick detrital flyschoid series (5 to 15 km), deposited through large alluvial fans. Those sediments, now forming the Songpan-Garzê accretionary prism were deposited on both the oceanic crust of the basin and the surrounding thinned continental margins (Zou *et al.* 1984; Sengör 1985; Rao & Xu 1987; Mattauer *et al.* 1992; Nie *et al.* 1994) (Figs 2b & 3).

During late Triassic–Lower Jurassic period, the Triassic Songpan-Garzê ocean is limited to the north by the Kunlun–Anyemaqen–Qinling subduction zone which induced the widespread emplacement of large calc-alkaline batholiths (220–200 Ma) (e.g. Roger *et al.* 2003, 2008) and controlled the development of the Kunlun and Qinling orogenic wedges. In the Qinling belt, continental subduction followed the oceanic closure, marked by late Triassic high-pressure metamorphism (Ames *et al.* 1993, 1996; Eide *et al.* 1994; Rowley *et al.* 1997; Hacker *et al.* 1998, 2006; Li *et al.* 2007) (Fig. 2c).

South of the Songpan-Garzê ocean deformation along the Jinsha subduction zone is attested by HP-LT, 220 Ma old blueschist metamorphism (Kapp *et al.* 2000; Pullen *et al.* 2008). At 210–200 Ma old calc-alkaline Yushu granites (Roger *et al.* 2003) were emplaced in the complex orogenic wedge bounding the northern edge of the Qiangtang block (Figs 1 & 4). To the SE, along the eastern margin of the Yidun block, a second series of calc-alkaline granites (219–216 Ma) was emplaced in late Triassic flysch-type sediments and volcanics (Reid *et al.* 2007) (Fig. 4).

Subduction under both the North China block and the Qiangtang block led to the shortening of

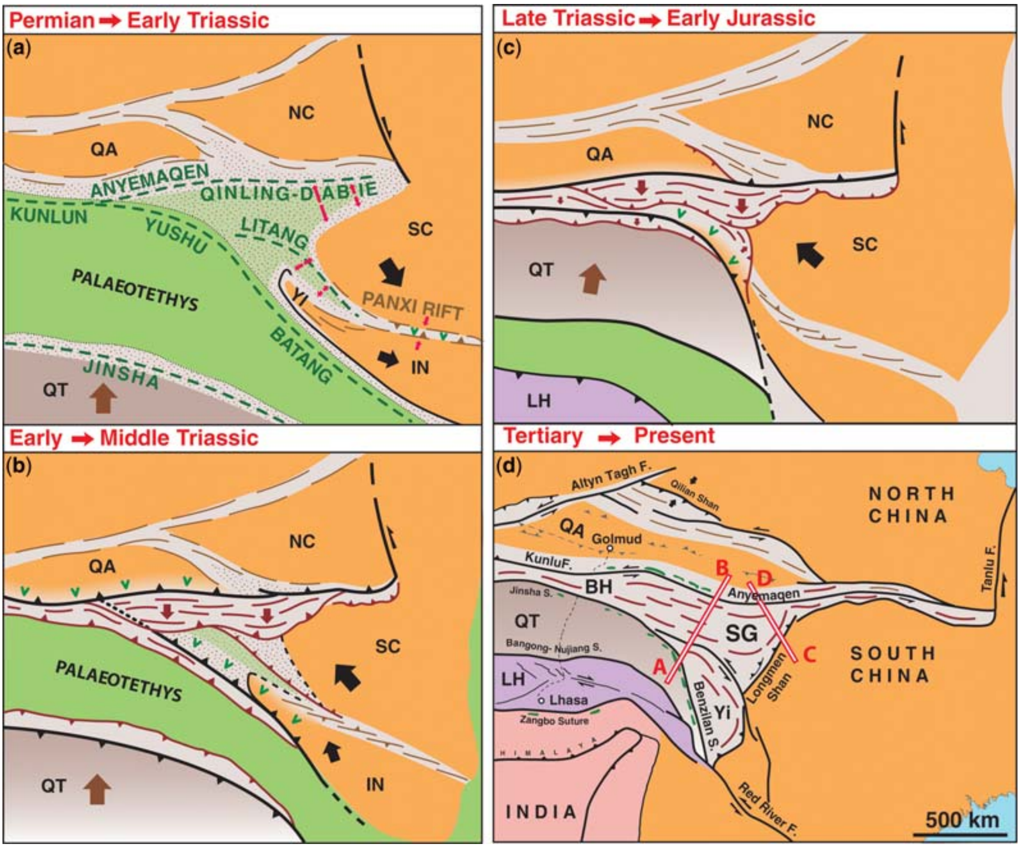

Fig. 2. Geodynamic evolution of North Tibet from Permian to Tertiary (modified after Roger *et al.* 2008, 2010). Dark green dotted lines show location and names of future subduction zones. Green area shows the Palaeotethysian domain and its northern branches (light green). Dotted area shows the domains of Triassic high sedimentary input. Yi, Yidun (or Litang-Batang) block; IN, Indochina block; QT, Qiangtang block; QA, Qaidam block; NC, North China block; SC, South China block; AB, CD location of evolutionary sections of Figure 3(a, b). (**a**) Northward motion of the Qiangtang block induces the closure of the Palaeotethys ocean and the development of the Yushu volcanic arc. (**b**) Shortening of the northeastern branch of the Palaeotethys ocean along the north-dipping Anyemaquen subduction zone. Growth of the Songpan-Garzê décollement – fold–thrust belt: the Songpan-Garzê prism is thrust onto the South China passive margin. (**c**) End of subductions: Remnants of the Palaeotethys (Jinsha suture) are trapped between the intra-oceanic Yushu arc/Yidun block and the Qiangtang continental margin. To the north, remnants of the northern oceanic basin (Anyemaquen suture) separate NC from the thick and wide Triassic orogenic wedge. (**d**) Shortening following the India–Asia collision induced south-verging continental subduction along the reactivated Jinsha suture zone. The Triassic décollement level is reactivated. Formation of the Longmen Shan initiates *c.* 30 Ma.

the Songpan-Garzê ocean and the development of the wide Triassic orogenic fold-thrust wedge (Figs 2–4). In the Songpan-Garzê area the Triassic series are intensively folded and separated from the crystalline basement outcropping near Danba by a large-scale south-verging décollement affecting the Palaeozoic series (Malavieille *et al.* 1991; Calassou 1994; Huang *et al.* 2003; Roger *et al.* 2004; Harrowfield & Wilson 2005; Zhou *et al.* 2008) (Fig. 4). The Triassic décollement zone has been recognized over more than 300 km and studied in detail in Tien Wan (SW of Konga Shan) and Danba areas (Mattauer *et al.* 1992; Xu *et al.* 1992; Calassou 1994; Harrowfield & Wilson 2005). However this structure or similar and/or associated ones can possibly be followed on thousands of kilometres from the north in the Dabie Shan and Qinling mountains to the south in the Konga Shan area (Hsü *et al.* 1987; Mattauer *et al.* 1992; Xu *et al.* 1992; Huang & Wu 1992; Calassou 1994; Roger *et al.* 2004; Harrowfield & Wilson 2005). The important shortening induced by the Triassic orogeny was accommodated through major crustal thickening of the orogenic wedge

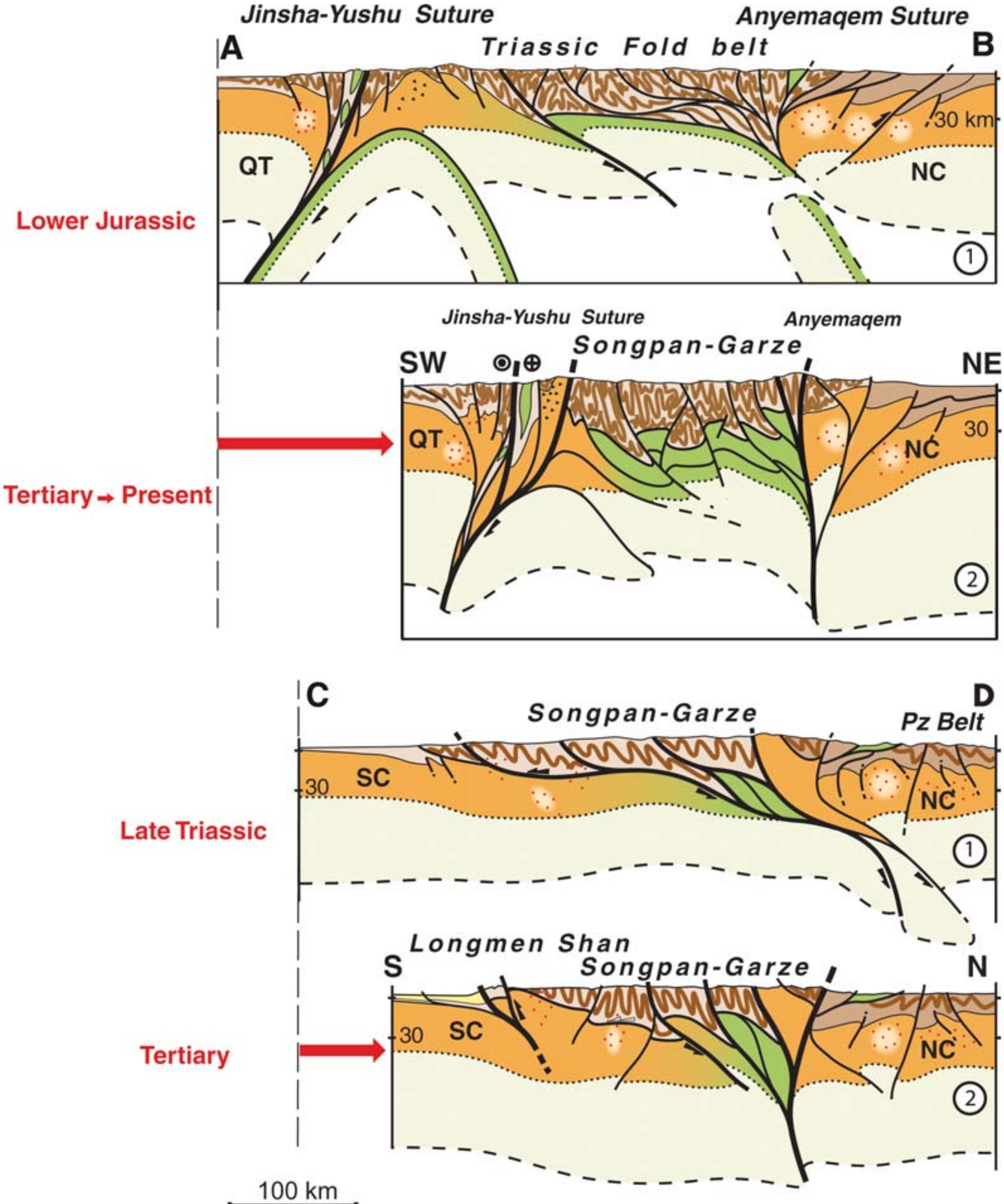

Fig. 3. Synthetic cross-sections showing the tectonic evolution of the Triassic belt from Jurassic–Tertiary (modified after Roger *et al.* 2008, 2010). See text and Figure 2 for detailed explanations.

(Malavieille *et al.* 1991; Calassou 1994; Roger *et al.* 2004) (Fig. 3). In the internal domain (close to Danba), this deformation is associated with a Barrovian type metamorphism (garnet–sillimanite–kyanite) (5–7 kbar and 400–600 °C) dated at 220–190 Ma (Xu *et al.* 1992; Huang *et al.* 2003; Zhou *et al.* 2008). Along the South China block passive margin, crustal thickening induced the emplacement of syn to late-orogenic adakitic or I-type and S-type granitoids (220–200 Ma) (Roger *et al.* 2004; Zhang *et al.* 2006; Xiao & Clemens 2007; Xiao *et al.* 2007). Later on, post-orogenic granitoids (200–150 Ma) were also emplaced into the prism (Wallis *et al.* 2003; Roger *et al.* 2004)

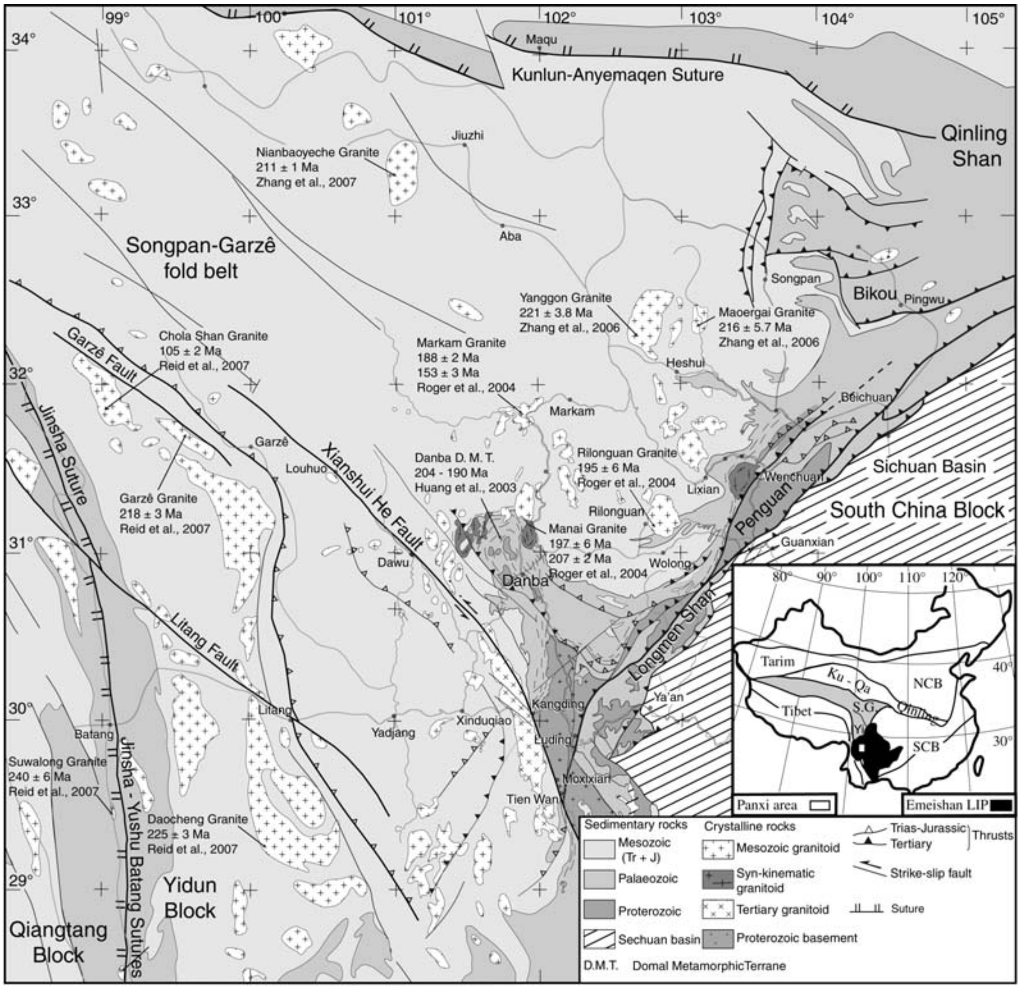

Fig. 4. Geological map of the Songpan-Garzê belt (modified after Roger *et al.* 2010 and C.I.G.M.R. 1991) showing the U–Pb ages available for the Triassic magmatic rocks and Danba domal metamorphic terrane (Danba D.M. T.).

(Fig. 4). The isotopic composition (Nd, Sr, Pb) of most of these granitoids shows that their magma source was predominantly derived from melting of the Songpan-Garzê Proterozoic basement (Yangtze block) with varying degrees of sedimentary material and negligible mantle source contribution (Roger *et al.* 2004; Zhang *et al.* 2006; Xiao *et al.* 2007). In the northern part of the Songpan-Garzê terrane, immediately south of the Anyemaqen suture zone, the Nianbaoyeche granite (211 $\pm$ 1 Ma) shows a different chemical composition (H. F. Zhang *et al.* 2007, 2008*b*) suggesting that the magma source is probably different (Fig. 4). The authors interpreted this granite as a post-orogenic A-type granite resulting from lithospheric delamination following the Triassic crustal thickening. However, the origin of the A-type granite is still debated. C. Z. Zhang *et al.* (2008*a*) proposed that the granite was generated by northward subduction along the Jinsha subduction zone. The very different isotope signature of the Nianbaoyeche granite compared to the other Sonpan-Garzê granites further south would seem instead to indicate a different origin, which might be related to the occurrence of a remnant oceanic crust below the sediments of the northern Songpan-Garzê basin (e.g. Roger *et al.* 2010) (Fig. 3).

Except for few localized Tertiary and Quaternary outcrops, post-Triassic sediments are totally absent from the Songpan-Garzê–Yidun fold belt (C.I.G.M.R. 1991) (Fig. 4). However, post-Triassic deformation has been recognized within the belt. During the Tertiary, it is generally admitted that additional shortening and crustal thickening has been induced by the India–Eurasia collision. It resulted in the Songpan–Garzê – Yidun area in a reactivation of the Triassic high angle faults, and folds, and large scale folding of the décollement of the accretionary belt. For instance, in the Danba area the décollement is affected by a wide Tertiary antiform with a NNW–SSE axis (Huang *et al.* 2003; Roger *et al.* 2004; Zhou *et al.* 2008). Still during the Tertiary, the décollement level has been exhumed in the hanging wall of the NE–SW thrust faults of the Longmen-Shan belt that marks the transition between the Tibetan Plateau and the Sichuan basin (Fig. 3). Toward the SW, the most prominent tectonic feature is the active sinistral strike slip Xianshui He fault (Allen *et al.* 1991). Geochronological data on the synkinematic Konga Shan granite have shown that the fault is active since at least the Miocene (13 Ma, U–Pb on zircons) (Roger *et al.* 1995) (Fig. 4). All this part of eastern Tibet have episodically absorbed significant shortening since the Late Triassic to present (Chen & Wilson 1996). The amount and precise timing of post-Triassic deformation in the Songpan-Garzê–Yidun and Longmen Shan area are difficult to constrain especially because of the difficulty to isolate the Tertiary thermochronological signal from the protracted Late Triassic–Cretaceous thermal history (e.g. Wilson *et al.* 2006). Nonetheless it is generally accepted that Jurassic–Cretaceous tectonism did not modified the general Triassic architecture of eastern Tibet (e.g. Burchfield *et al.* 1995; Roger *et al.* 2004; Harrowfield & Wilson 2005; Reid *et al.* 2005*b*; Wilson *et al.* 2006).

In the following the thermal evolution of eastern Tibet is presented and discussed in detail. First using a simple 1-D thermal modelling, we pay a special attention to Cretaceous thermal structure to estimate the parameters-set that could lead to the stable thermal regime observed over 100 Ma. Next, based on available low temperature thermochronological data we study the timing and the location of late tertiary exhumation. Finally we discuss the tectonic implications on the evolution of eastern Tibet over the last 200 Ma.

Pre-Tertiary cooling curves: 100 Ma of thermal quiescence

The Songpan-Garzê prism: an atypical belt?

Geochronological data account for the closure temperature of each mineral/geochronological system (Dodson 1973). Figures 5 and 6 present general cooling curves drawn using ages obtained from various geochronometers applied to single samples of granites and gneisses from south Songpan-Garzê (Xu & Kamp 2000; Kirby *et al.* 2002; Roger *et al.* 2004; Zhang *et al.* 2006), western Kunlun (Arnaud *et al.* 2003; Jolivet *et al.* 2003; Roger *et al.* 2003) and Yidun arc (Reid *et al.*, 2005*a*, 2007; Lai *et al.* 2007). The cooling curves obtained for these three Triassic granites are similar: a phase of rapid cooling immediately after the emplacement of the pluton, followed by a very slow and regular cooling during Late Jurassic and Cretaceous–Early Tertiary. Together these results suggest: (1) that the initial rapid cooling rate during the Late Triassic was induced by a large thermal contrast between the newly emplaced granite body and the sedimentary rocks rather than by a high exhumation rate; and (2) an absence of major tectonic events between *c.* 150 and 50–30 Ma. The fission tracks (zircons) data (Xu & Kamp *et al.* 2000; Kirby *et al.* 2002; Lai *et al.* 2007) indicate that the final exhumation and Tertiary cooling is younger than 30 Ma. Richardson *et al.* (2008) demonstrated the occurrence of a major, general erosion event in the Sichuan basin initiating after 40 Ma and no later than 25 Ma. They rely this phase of major erosion (at least 1.3 km of sediments removed) to major modifications of the drainage pattern and especially the driving of the Middle and Lower Yangtze Rivers through the Three Gorges area. Such reorganization of the drainage pattern could also indicate the onset of topography building in northeastern Tibet.

In the South Songpan-Garzê area, the temperature prevailing for each sample during the thermal stability period can be directly related to their burying depth at the onset of this thermal phase. For example, the post-tectonic Markam granite, mainly derived from melting of the Songpan Garzê sediments was emplaced *above* the décollement level and shows a temperature of stability (i.e. the temperature from which the observed cooling curve becomes nearly flat for a long period of time, temperature corresponding to an equilibrium with the host rock) around 300 °C, whereas the syntectonic Manai granite which was emplaced inside the décollement level shows a temperature of stability of 500 °C (Figs 5 & 6a). Finally the Yanggon and Maoergai granites were emplaced higher up in the sedimentary pile at temperatures of 200–300 °C (Figs 5 & 6a).

The cooling history of the major metamorphic zones in the ‘Danba Domal Metamorphic Terrane’ is similar to that of the Manai granite. Huang *et al.* (2003) interpreted these geochronological data as a two-stages metamorphic evolution in the Danba high-grade metamorphic terrane. The Barrovian metamorphic phase M1 (garnet, staurolite, and kyanite zones) (5–7 kbar and 570–600 °C) initiated at the end of the Triassic due to the collision between the South China and North China blocks.

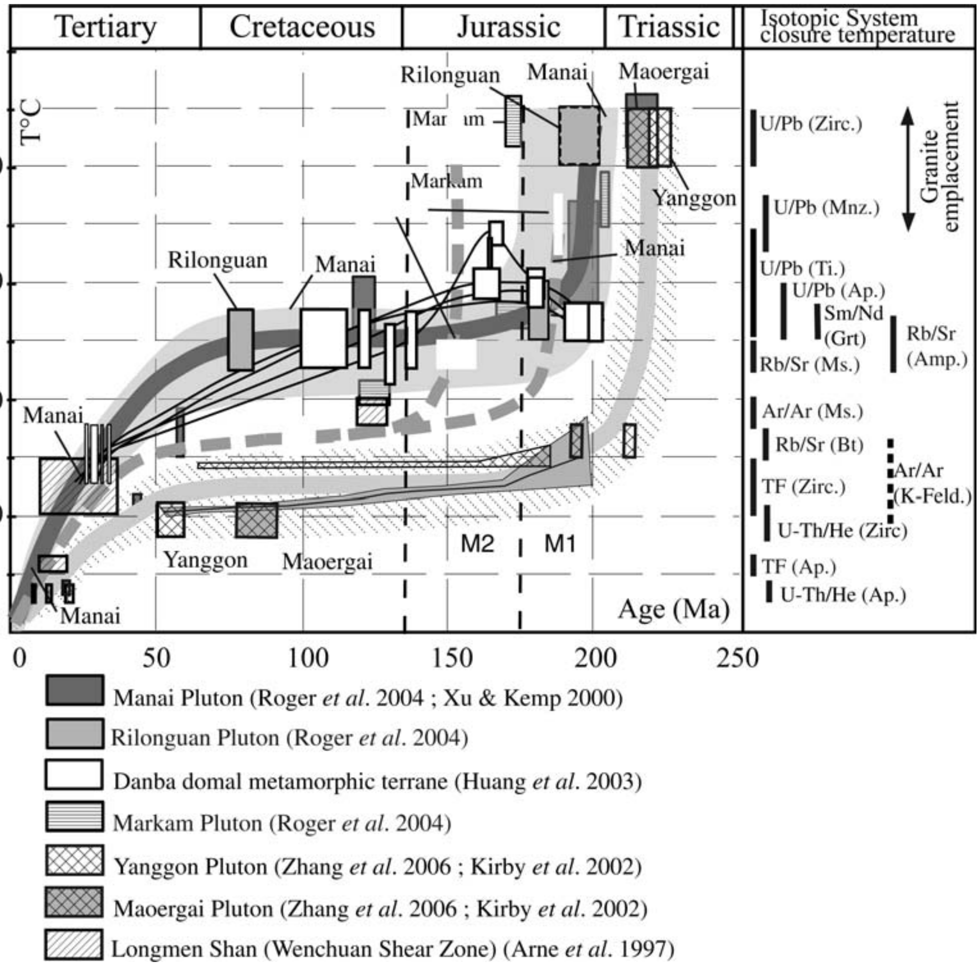

Fig. 5. Compilation of geochronological data obtained on magmatic and sedimentary rocks in the South Songpan-Garzê. All cooling histories display a similar trend. The grey envelope shows the cooling history of the Ma Nai and Rilonguan granites as well as of metamorphic rocks in the Danba area (white boxes). Rapid cooling after granite emplacement is followed by a very slow and regular cooling during Jurassic and Cretaceous, suggesting the absence of major tectonic events between *c.* 150 and 50–30 Ma. The fission tracks (TF) data indicate that the final exhumation and cooling occurred around 30 Ma. U–Pb and Rb/Sr data are from Roger *et al.* (2004), and the fission track data are from Xu & Kamp (2000). Danba data are from Huang *et al.* (2003). The striped boxes represent the data from the Markam granite. The hatched envelope shows the cooling history of the Yanggon and Maoergai granites. U–Pb data are from Zhang *et al.* (2006) and Kirby *et al.* (2002). Rb–Sr (biotite), Ar/Ar (K-feldspar) and U–Th/He (apatite and zircon) data are from Kirby *et al.* (2002). Closure temperatures used are estimated (excepted for some metamorphic data). Zirc., zircon; Mnz, monazite; Ti, titanite; Ap., apatite; Gr, garnet; Amp., amphibole; Ms, muscovite; Bt, biotite; K-Feld., K-feldspar.

M1 was recorded throughout the Songpan-Garzê orogenic belt with peak conditions reached at 204–190 Ma. The second higher-temperature sillimanite-grade M2 metamorphic phase (660–725 °C) occurred locally in the northern Danba area at 164 Ma. It is marked by the occurrence of sillimanite and local migmatite and may represent a local thermal perturbation. The origin of this event remains unclear. For Huang *et al.* (2003) the M2 thermal event could have been related to east–west compression during the early Yenshanian collision between the south Tibet (Lhasa terrane) and north Tibet blocks. But recently, Zhou *et al.* (2008) proposed that the Neoproterozoic crystalline basement of Danba was first exhumed in Middle Jurassic (159–173 Ma) during the beginning of a

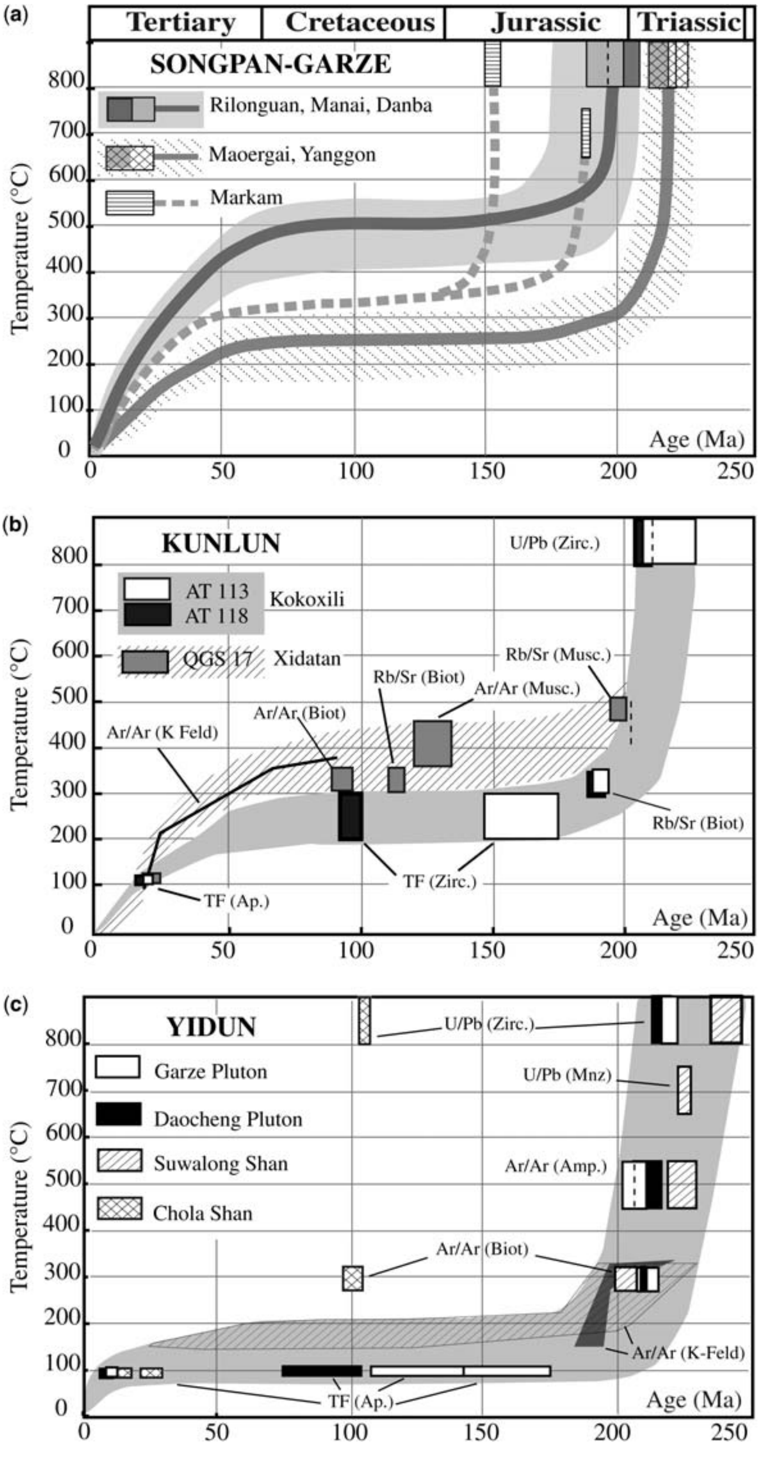

Fig. 6. Cooling histories of (**a**) the South Songpan-Garzê rocks (see Fig. 5 for details of the data), (**b**) the Kunlun granites and gneiss and (**c**) the Yidun arc granites drawn from multisystem geochronology. For the Kunlun area (b), two Kokoxili sample are Triassic granites (White and black box). Data are from Roger *et al.* (2003) and Jolivet *et al.* (2003). For the Xidatan orthogneiss (grey box), the data are from Arnaud *et al.* (2003). These areas have a similar cooling history. For the Yidun granites, the data are from Reid *et al.* (2005*a*, 2007) and Lai *et al.* (2007).

major period of extensional deformation in the region generated by the collision between the north China and south China blocks. Between 138 and 30 Ma, cooling appears uniform and slow. Clustered Rb–Sr biotite ages mark a return to fast cooling rates (associated to renewed uplift and exhumation) around 30 Ma (Huang *et al.* 2003) (Fig. 5).

The *c.* 100 Ma long period of thermal stability observed in all the cooling curves presented in Figure 6 suggests a lack of major tectonic event, erosion or sedimentation between *c.* 150 and *c.* 30 Ma (Xu & Kamp 2000; Jolivet *et al.* 2001; Kirby *et al.* 2002, Huang *et al.* 2003, Roger *et al.* 2003, 2004, 2010, Reid *et al.* 2005*a*,*b*, 2007; Lai *et al.* 2007; Zhou *et al.* 2008). This near absence of thermal change is not restricted to the cooling history of the Triassic granites but is also recorded by the metamorphic series of the Danba dome (Figs 5 & 6a) or by some Palaeozoic granites in the Kunlun belt (Xidatan orthogneiss) (Fig. 6b). Furthermore, all these samples have very different geodynamical settings: crustal thickening in Songpan-Garzê, subduction related calc-alkaline magmatism in the Kunlun and Yidun (Roger *et al.* 2003, 2004; Reid *et al.* 2005*a*,*b*, 2007; Zhang *et al.* 2006).

In the Yidun block, the emplacement of the Cretaceous granites (Chola Shan granite; Reid *et al.* 2007) does not affect the thermal history of the Indosinian plutons (Fig. 6c). Furthermore, after a very rapid cooling following their emplacement, those younger granites reach the same temperature of stability as the Indosinian ones. This confirms that the emplacement of the Cretaceous granites is not related to a tectonic episode and that they cannot be used to support a Cretaceous Yenshan tectonic event in Kunlun, Yidun or Songpan Garzê (Dirks *et al.* 1994; Chen *et al.* 1995; Arne *et al.* 1997; Arnaud *et al.* 2003). On the northern side of the Qinling ranges to the NE, fission track and K-feldspar $^{40}Ar/^{39}Ar$ data indicate rapid cooling and local strong exhumation (over 4 km) during Late Cretaceous, mostly associated with local basin formation and strike–slip fauling (Ratschbacher *et al.* 2003; Enkelmann *et al.* 2006). Further east, in Dabie Shan, apatite fission track ages are also Late Cretaceous. Finally, Vincent & Allen (1999) reported evidences of local Late Jurassic–Early Cretaceous north–south transtensive movements in the Hexi corridor along the eastern edge of the Qilian Shan. Evidences for Cretaceous exhumation and tectonic movements are thus obviously found east and NE of the actual Tibet plateau. However Cretaceous exhumation is generally localized, mostly associated with strike–slip faults and small-scale extensional basins. The Cretaceous sedimentation in the Sichuan basin is represented by lacustrine and aeolian series indicative of a general low sediment input (see synthesis in Richardson *et al.* 2008). All these observations associated with the cooling curves presented above seem to indicate that, if the Yenshan event did exist, it only affected eastern China and not the Tibet plateau area. In that respect it is difficult to link this event to the Lhasa–Qiangtang collision.

Numerical modelling

The thermal structure of the lithosphere depends on many factors, including the boundary conditions, surface erosion and material properties. Here we only focus our approach on the very slow cooling rate between Late Jurassic and Early Cenozoic obtained from granites of South Songpan-Garzê and Kunlun.

Assuming negligible horizontal heat transfer, we use a simple 1D thermal modelling that takes into account the thermal properties of both sediments and crust within these areas (Fig. 7). Furthermore we assume that the dominant thermal processes are radiogenic heat production and conductive heat transport towards the surface. The temperature T as a function of time t and depth z is thus given by the following transient heat equation

$$\frac{\partial T}{\partial t} = \frac{1}{\rho C_P}\left(k\frac{\partial^2 T}{\partial z^2} + A\right) - v_z\frac{\partial T}{\partial z}, \qquad (1)$$

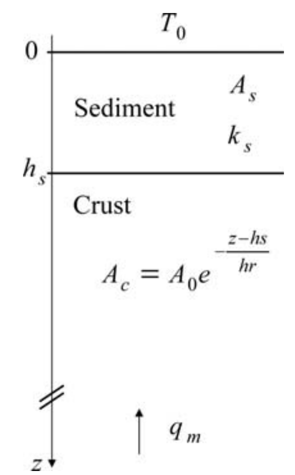

Fig. 7. Physical model setup showing the boundary conditions and material properties used in this study. T_0 is the surface temperature. q_m is the upward heat flux at the base of the model. A_s, A_c, A_0, h_r, k_s and h_s are the sedimentary heat production, the crustal heat production, the heat production at the top of the crust, the exponential decay of the crustal heat production, the sedimentary thermal conductivity and the sediment thickness, respectively.

where ρ is the density, C_P the heat capacity, k the thermal conductivity, A the radiogenic heat production and v_z the vertical advection associated to exhumation. Here we study a long time period (at least 100 Ma) of very low cooling rate. The lack of post-Triassic sediments in the Songpan-Garzê area, the occurrence of a complete Jurassic to Quaternary section within the present-day surrounding basins (Sichuan and Qaidam), and a Jurassic to Cretaceous sequence on the Qiangtang block suggest that this low cooling rate can be related to very low erosion rates.

In the following we consider an end-member model with a steady state temperature field ($\partial T/\partial t = 0$) and no denudation processes ($v_z = 0$). The equation 1 becomes

$$0 = k\frac{d^2T}{dz^2} + A, \tag{2}$$

that can be easily solved to interpret the Cretaceous temperature field. For sediments we assume a constant thermal conductivity k_s ranging from $1-5\ \mathrm{W\ m^{-1}\ K^{-1}}$ and we take constant heat production A_s between $0-5\ \mu\mathrm{W\ m^{-3}}$ Following Turcotte & Schubert (2002) we assume that crustal heat production decreases exponentially with depth

$$A_c = A_0 e^{-(z-h_s)h_r} \tag{3}$$

with h_s the thickness of the sedimentary layer, A_0 the radiogenic heat production at the top of the crust ($z = h_s$) and h_r a length scale for the decrease in A_c with depth. We take $A_0 = 0-5\ \mu\mathrm{W\ m^{-3}}$ and $h_r = 5-15$ km (Turcotte & & Schubert 2002). Integration of equation 2 using the boundary conditions $T_0 = 0\ ^\circ\mathrm{C}$ at $z = 0$ km and upward heat flux $q_\mathrm{m} = 15-30\ \mathrm{mW\ m^{-2}}$ at great depth ($z \rightarrow +\infty$) gives for temperature field within the sedimentary layer

$$\mathrm{T} = -\frac{1}{2}\frac{A_s}{k_s}z^2 + \frac{q_m + A_0\,h_r + A_s h_s}{k_s}z + T_0. \tag{4}$$

First for granites of south Songpan-Garzê we use this last equation to calculate the depth of both Markam mica granite and Manai and Rilonguan amphibole granites associated with Cretaceous temperatures of 300–400 °C and 450–550 °C, respectively (Roger *et al.* 2004). Based on earlier studies (Xu *et al.* 1992; Calassou 1994) we assume a sediment thickness $h_s = 15-30$ km. We obtained two Gaussian distributions of depth with means $\mu_{300-400^\circ\mathrm{C}} = 12.5$ km and $\mu_{450-550^\circ\mathrm{C}} = 20$ km associated with standard deviations $\sigma_{300-400^\circ\mathrm{C}} =$ 3 km and $\sigma_{450-550^\circ\mathrm{C}} = 5$ km, respectively. Next, using these distributions we estimate the *a posteriori* distribution of thermal parameters (Fig. 8). A wide range of modelling gives a good agreement between estimated and calculated temperature. We show that crustal parameters A_0, h_r as well as q_m are poorly constrained. Not surprisingly, our result confirms that thermal properties of sediments have a primary control on the temperature field within the sedimentary layer. We obtain high heat production $A_s = 3-4\ \mu\mathrm{W/m^3}$, high thermal conductivity $k_s = 3.5-4.5$ W/m and a sediment thickness of at least 23 km, which is consistent with the depth of emplacement of granites inferred from metamorphic studies (Xu *et al.* 1992).

A similar approach is used to interpret Kokoxili and Xidatan granites along the western Kunlun fault, which gives Cretaceous temperature of 200–300 and 300–450 °C, respectively (Fig. 6). As for the Songpan-Garzê, the calculated temperatures are mostly controlled by sedimentary properties. Thus our inversion cannot be used to estimate crustal parameters (Fig. 9). For sediment more than 65% of the models give a high heat production $A_s > 3-4\ \mu\mathrm{W/m^3}$ and a thermal conductivity $k_s = 2-3.5$ W/m. The calculated distribution of sediment thickness shows that h_s is mostly controlled by the *a priori* information on depth, which gives a pressure <3.5 kbar for metasediments (Harris *et al.* 1988).

Together the results obtained from the Songpan-Garzê and Kunlun granites suggests that: (1) high temperature can be maintained over a long period of time; and (2) Cretaceous cooling temperature is mostly controlled by the thermal properties of sediments of continental origin.

Discussion and tectonic implications

Our results demonstrate that a reasonable combination of high thermal conductivity and high heat production in the sediments is able to account for the observed Cretaceous thermal quiescence in the south Songpan-Garzê terrane as well as in western Kunlun (Fig. 10). It demonstrates that whatever the nature of the crust, high thermal steady state can be maintained over such a long time period of thermal stability. The continental nature of the underlying crust within the southern part of the Songpan-Garzê belt is widely accepted. The geochemistry of the I-type and adakitic-type granites clearly demonstrates that they are essentially derived from partial melting of a Neoproterozoic crystalline basement similar to the basement of the Yangtze craton (Roger *et al.* 2004; Zhang *et al.* 2006). However, within the northern part of the prism, east of the Longmen Shan, the nature of the crust is still debated as no outcrop is available (Zhang *et al.* 2007; Roger *et al.* 2008, 2010). We recently proposed that the peculiar tectonic

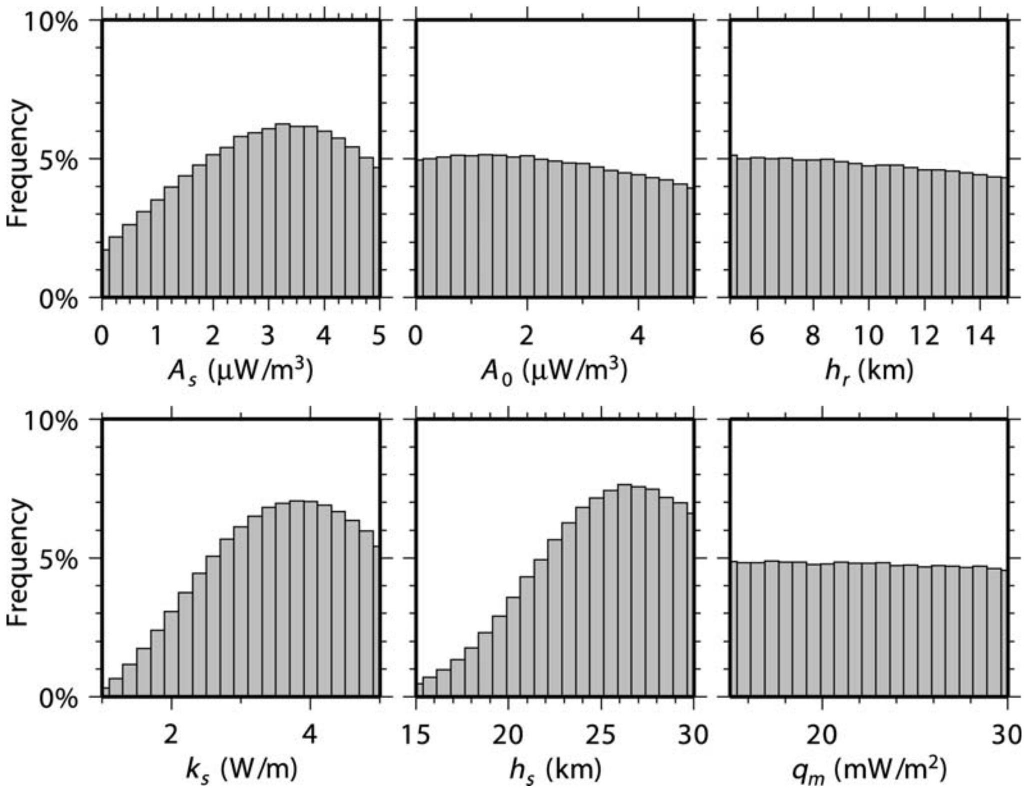

Fig. 8. *A posteriori* distribution of thermal parameters obtained from the inversion of Cretaceous temperature estimated in south of Songpan-Garzê. A_s, A_0, h_r, k_s, h_s and q_m are respectively the sedimentary heat production, the heat production at the top of the crust, the exponential decay of the crustal heat production, the sedimentary thermal conductivity, the sediment thickness and the upward heat flux at the base of the model. The range of each parameter is given *a priori* from available geological and metamorphic data.

and geodynamic setting of the Songpan-Garzê basin and surrounding blocks did not allow a complete collision between the main continental domains (Roger *et al.* 2008, 2010). The volumes of Triassic sediments deposited in the basin are huge and the series are exceptionally thick (up to 25 km). Associated to the triangular geometry of the convergence zone between the Qiangtang, south China and Kunlun/north China blocks that thickened the series it led, during the orogenesis, to the build-up of a wide accretionary orogen. However we propose that the converging system gets blocked before the complete subduction of the Songpan-Garzê oceanic crust. We currently do not have enough data to build up the complete cooling curve for any granite in north Songpan-Garzê. However, our physical modelling shows that the nature of the underlying crust has no or minor effect in the thermal evolution of the samples. This implies that the shape of the obtained cooling curve in north Songpan-Garzê and in the other parts of the study area should be similar. The only unknown parameter remains the depth of the granites during the thermal stability period.

Furthermore our modelling suggests that the main parameter controlling the temperature stability is the sediment thickness that must remain constant over a long period of time (100 Ma). This supports the assumption that sedimentation and erosion were not active in the area from Late Triassic–Early Tertiary. The 20–25 km of sediments required to maintain the Manai and Rilonguan samples at a temperature of 500 °C during the period of thermal stability correspond to the generally accepted sediment thickness within the Songpan-Garzê prism (Mattauer *et al.* 1992; Xu *et al.* 1992; Calassou 1994; Roger *et al.* 2008, 2010) (Fig. 8). As already suggested above, the lower temperature of stability of the Markam granite (300 °C) is explained by the position of the granite further up in the sedimentary sequence. In the Kunlun belt the temperature of stability

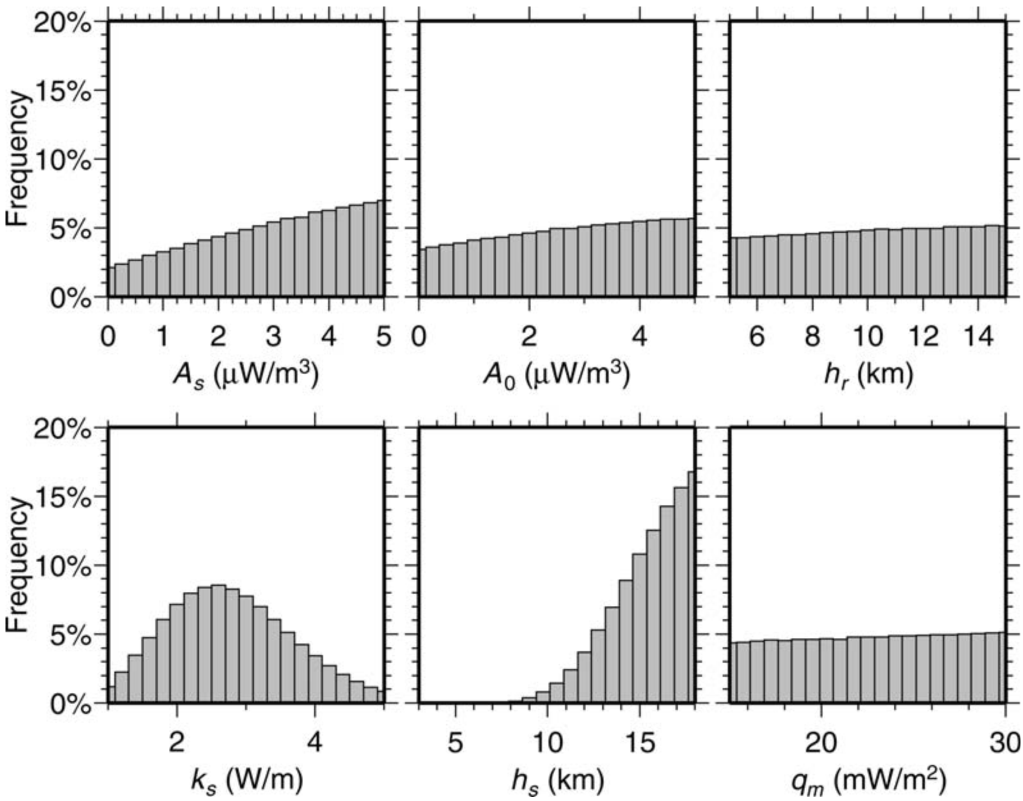

Fig. 9. Same as Figure 8 for western Kunlun.

of the samples is *c.* 300–400 °C similar to the temperature observed in Markam. In the Yidun block, the temperature of stability is much lower, *c.* 100 °C suggesting a thinner sedimentary cover (Figs 6 & 10).

Late Tertiary, localized reactivation of the exhumation

The Tertiary deformation that affected the Songpan-Garzê prism, and especially the growth of the Longmen Shan range is difficult to date and characterize. From a tectonic and metamorphic point of view, the Tertiary deformation was strongly influenced by the Indosinian and older structures, so that it is difficult to unravel the effects of the Cenozoic deformation from the Triassic deformation (e.g. Calassou 1994; Roger *et al.* 2008). Along the Longmen Shan, the large drop in altitude between the 4000 m high plateau and the 500 m high Sichuan basin is correlated with a sharp variation in the Moho depth, from 55 to 60 km below the plateau to 40 km in the Sichuan basin (Wang *et al.* 2007; Xu *et al.* 2007; Robert *et al.* 2010). While part of this structure must be correlated to the Late Miocene uplift (e.g. Clark *et al.* 2005*b*) part of it could be inherited from the Triassic orogeny. Near Danba, the Triassic décollement level is refolded by a large antiformal structure NNW–SSE axis that could correspond to Tertiary folding. Similarly within the Longmen Shan, the NE–SW-trending faults that separate the plateau from the Sichuan basin have absorbed significant shortening between Late Triassic and present (Chen & Wilson 1996). Finally, activity along the major Xianshui He strike–slip fault is attested by shearing of the syn-tectonic, 13 Ma old Konga Shan granite (Roger *et al.* 1995) (Fig. 11).

Low temperature thermochronology (fission tracks and U–Th/He) data available in south Songpan-Garzê, Yidun and Longmen Shan (Figs 6 & 11) indicate that the final exhumation and cooling occurred in the Tertiary after *c.* 30–25 Ma (Arne *et al.* 1997; Xu & Kamp 2000; Jolivet *et al.* 2001; Kirby *et al.* 2002; Huang *et al.* 2003; Roger *et al.* 2004; Wilson *et al.* 2006; Lai *et al.* 2007). This exhumation episode can be separated in two

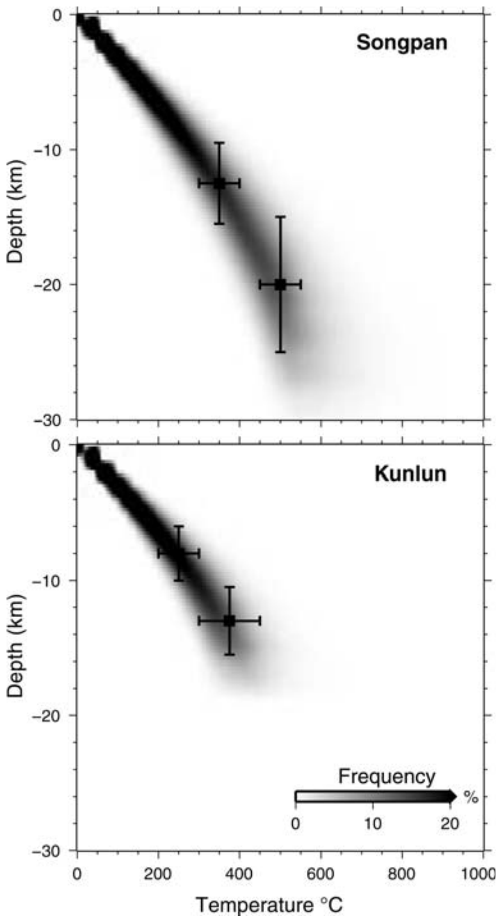

Fig. 10. Temperature field at depth within the sedimentary layer. Grey scale gives the 'likelihood' of the calculated geotherm. Top: Black squares give the estimated temperature of mica granite and amphibole granite of south Songpan-Garzê. Bottom: Black squares give the estimated temperature of Kokoxili and Xidatan granites of western Kunlun.

phases: a regional moderate cooling starting *c*. 25 Ma followed by a second, stronger phase initiating between *c*. 10 and 5 Ma (Roger *et al.* 1995; 2004; Arne *et al.* 1997; Xu & Kamp 2000; Kirby *et al.* 2002; Wilson *et al.* 2006; Zheng *et al.* 2006; Lai *et al.* 2007). Figure 11 displays a compilation of the available apatite fission track data grouped in age intervals. The resulting image indicates that the Tertiary exhumation is restricted along the major tectonic features such as the Xianshui He fault or the Longmen Shan range. Away from these structures the Tertiary exhumation is nearly null or at least too weak to have been registered by the thermochronometer. For example, the Garzê and Daocheng granite plutons have apatite fission track ages older than 100 Ma (Lai *et al.* 2007) implying that these areas were not or only weakly affected by post-Jurassic exhumation (Fig. 11). Furthermore, the ages obtained from the Daocheng pluton tend to decrease while approaching the Garzê and Litang thrust faults to the east. This trend is further confirmed by the ages between 10–25 Ma obtained immediately along the active Garzê and Litang strike–slip faults (Lai *et al.* 2007) (Fig. 11). Within the Min Shan, the apatite fission track ages range between 30–100 Ma with the exception of one sample with an age of 122 ± 12 Ma near Songpan (Arne *et al.* 1997). Like in the Garzê–Litang area, the ages tend to be younger close to the prominent tectonic features such as the Min Shan thrust fault or the edge of the northern Longmen Shan range. (U–Th)/He data indicate that thrusting along the Min Shan thrust fault, west of Songpan is thought to initiate *c.* 5–3 Ma leading to renewed erosion (Kirby *et al.* 2002). We thus interpret the fission track ages in that region as intermediate between the Mesozoic ages obtained on the Garzê and Daocheng plutons as well as in Songpan, and the truly Tertiary ages associated to the last exhumation episode.

The onset of thrusting along the Min Shan fault is coeval with the second phase of increased exhumation that is only observed (with the exception of 2 samples near the Yushu-Batang suture zone) along the easternmost major tectonic structures (Xianshui He fault, Jinsha thrust, Longmen Shan thrust system and the Songpan-Garzê Triassic décollement fault) (Roger *et al.* 1995, 2004; Arne *et al.* 1997; Xu & Kamp 2000; Kirby *et al.* 2002; Wilson *et al.* 2006; Lai *et al.* 2007). This last exhumation episode is confirmed by the few (U–Th)/He data available along the Longmen Shan (Kirby *et al.* 2002; Godard *et al.* 2009). Within the Longmen Shan range, a total denudation of 7–10 km is estimated for the late Cenozoic period (Arne *et al.* 1997; Kirby *et al.* 2002; Clark *et al.* 2005*a*,*b*). Similar amounts of late Tertiary denudation have been estimated along an east–west section across the Xianshui He fault near Kangding: west of the fault, the denudation reaches 4–6 km east of the fault and 7–10 km west of the fault (Xu & Kamp 2000). Figure 11 also shows that the Triassic décollement level is reactivated leading to the exhumation of the Manai and Rilonguan granites. Similarly, however based on very few data, thrusting along the Batang suture zone may also be reactivated probably because these north–south trending faults are perpendicular to the regional direction of compression. This is again indicative of the strong influence of the inherited structures on the ongoing deformation. The second exhumation phase is not imaged along the western half of the Xianshui He

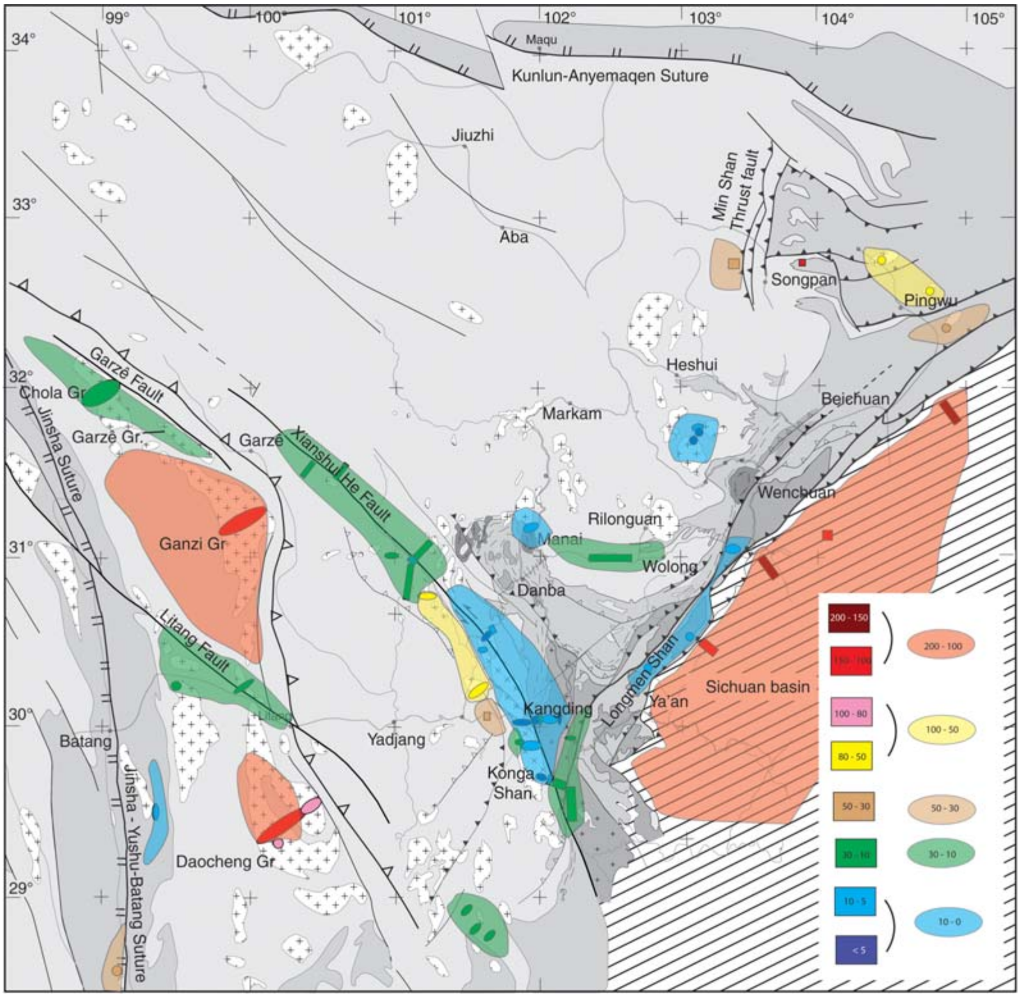

Fig. 11. Geological map of the Songpan-Garzê belt (modified after Roger *et al.* 2008, 2010 and C.I.G.M.R. 1991) showing the fission track ages (apatite) available for the Triassic magmatic and sedimentary rocks grouped into time spend corresponding to the main geodynamic phases. Individual data are indicated below the general envelopes. See text for discussion. Data are from Arne *et al.* (1997), Xu & Kamp (2000), Reid *et al.* (2005*a*), Zheng *et al.* (2006) and Lai *et al.* (2007).

fault or along the Litang and Garzê faults, probably because these are nearly pure strike–slip and do not create much relief.

The Tertiary exhumation (caused by compressional tectonics) thus appears mostly concentrated along the limit between the plateau and the Sichuan basin, the former being squeezed on the later since *c.* 30–25 Ma with a increased activity since less than 10 Ma. The internal part of the Songpan-Garzê prism is poorly exhumed as Mesozoic low temperature thermochronology ages are preserved, probably due to a very distributed Tertiary shortening (and thickening) in most part of the huge Triassic sedimentary accretionary belt that constituted the eastern part of the Tibetan Plateau.

Conclusion

Complete cooling curves of basement rocks and syn- to post-tectonic granite throughout the whole north-eastern Tibet area demonstrate that, while the Indosinian orogeny that led to the building of the Songpan-Garzê thrust and fold belt was a major geodynamic episode, it has been followed by a very long period of stability. For *c.* 100 Ma, between Late Jurassic–Middle Tertiary, deformation as well as erosion and sedimentation were very low and distributed. This implies that the accretion of the Lhasa block during the Cretaceous had, if any, only a very limited effect on the tectonic, metamorphic and topographical structure of north and north-eastern Tibet. Between the end of the Indosinian orogeny and the onset of the Tertiary deformation at *c.* 30 Ma, the Songpan-Garzê area remained probably a flat and poorly drained region. While we have no indication of its absolute elevation, the lack of Jurassic–Tertiary sediments suggests that the Triassic belt already constituted a plateau higher than the surrounding basins. Finally the low temperature thermochronological data indicate that the Tertiary deformation allows exhumation only where it is strongly localized, i.e. along inherited tectonic structures. This result underlines the need of studying the pre-Tertiary tectonic evolution to understand the present-day deformation pattern and tectonic activity.

The authors would like to thank all the colleagues involved in the field expeditions which took place between 1990 and 2000, particularly the leaders Z. Q. Xu, P. Tapponier and M. Mattauer. Most of these studies were supported by INSU–CNRS funding. Special thanks go to E. Kirby and an anonymous reviewer for their comments and suggestions.

References

ALLEN, C. R., QIAN, H., WEN, X., ZHOU, H. & HUANG, W. 1991. Field study of a highly active fault zone: the Xianshui He fault of Southwestern China. *Geological Society of America Bulletin*, **103**, 1178–1199.

AMES, L., TILTON, G. R. & ZHOU, G. Z. 1993. Timing of collision of the Sino-Korean and Yangtse cratons: U–Pb zircon dating of coesite-bearing eclogites. *Geology*, **21**, 339–342.

AMES, L., ZHOU, G. & XIONG, B. 1996. Geochronology and isotopic character of ultrahigh-pressure metamorphism with implications for collision of the Sino-Korean and Yangtze craton, central China. *Tectonics*, **15**, 472–489.

ARNAUD, N., TAPPONNIER, P., ROGER, F., BRUNEL, M., SCHÄRER, U., CHEN, W. & XU, Z. 2003. Evidence for Mesozoic shear along the western Kunlun and Altyn-Tagh fault, northern Tibet (China). *Journal of Geophysical Research*, **108**, 2053–2080, doi: 10.1029/2001JB000904.

ARNE, D., WORLEY, B. *ET AL.* 1997. Differential exhumation in response to episodic thrusting along the eastern margin of the Tibetan Plateau. *Tectonophysics*, **280**, 239–256.

BURCHFIELD, B. C., CHEN, Z., LIU, Y. & ROYDEN, L. H. 1995. Tectonics of the Longmen Shan and adjacent regions, Central China. *International Geology Review*, **37**, 661–735.

CALASSOU, S. 1994. *Etude tectonique d'une chaîne de décollement: (a) tectonique triasique et tertiaire de la chaîne de Songpan-Garzê. (b) géométrie et cinématique des déformations dans les prismes d'accrétion sédimentaires: modélisation analogique*. PhD thesis, University of Montpellier II, France.

CHEN, S. F. & WILSON, C. J. L. 1996. Emplacement of the Longmen Shan Thrust-Nappe Belt along the eastern margin of the Tibetan Plateau. *Journal of Structural Geology*, **18**, 413–440.

CHEN, S. F., WILSON, C. J. L. & WORLEY, B. A. 1995. Tectonic transition from the Songpan-Garzê fold belt to the Sichuan basin, south-western China. *Basin Research*, **7**, 235–253.

C.I.G.M.R. (Chengdu Institute of Geology and Mineral Resources) 1991. Geological Map of Xinghai-Xizang (Tibet) Plateau and adjacent areas (1:1 500 000) and Explanatory Note. Chengdu Cartographic Press, Chengdu.

CLARK, M. K., BUSH, J. W. M. & ROYDEN, L. H. 2005*a*. Dynamic topography produced by lower crustal flow against rheological strength heterogeneities bordering the Tibetan Plateau. *Geophysical Journal Interior*, **162**, 575–590.

CLARK, M. K., HOUSE, M. A., ROYDEN, L. H., WHIPPLE, K. X., BURCHFIELD, B. C., ZHANG, X. & TANG, W. 2005*b*. Late Cenozoic uplift of eastern Tibet. *Geology*, **33**, 525–528, doi: 10.1130/G21265.1.

DIRKS, P. H. G., WILSON, C. J. L., CHEN, S., LUO, Z. L. & LIU, S. 1994. Tectonic evolution of the NE margin of the Tibetan Plateau: evidence from the central Longmen Moutains, Sichuan Province. *Journal of Southeast Asian Earth Sciences*, **9**, 181–192.

DODSON, M. H. 1973. Closure temperature in cooling geochronological and petrological system. *Contribution to Mineralogy and Petrology*, **40**, 259–274.

EIDE, E. A., MCWILLIANS, M. O. & LIOU, J. G. 1994. $^{40}Ar/^{39}Ar$ geochronology and exhumation of high-pressure to ultrahigh pressure metamorphic rocks in east-central China. *Geology*, **22**, 601–604.

ENKELMANN, E., RATSCHBACHER, L. *ET AL.* 2006. Cenozoic exhumation and deformation of northeastern Tibet and the Qinling: Is Tibetan lower crustal flow diverging around the Sichuan Basin? *GSA Bulletin*, **118**, 651–671; doi: 10.1130/B25805.1.

GODARD, V., PIK, R. *ET AL.* 2009. Late Cenozoic evolution of the central Longmen Shan, eastern Tibet: Insight from (U-Th)/He thermochronometry. *Tectonics*, **28**, 5, TC5009, doi: 10.1029/2008TC002407.

HACKER, B. R., RATSCHBACHER, L., WEBB, L., IRELAND, T., WALKER, D. & SHUWEN, D. 1998. U/Pb zircon ages constrain the architecture of the ultrahigh-pressure Qinling-Dabie Orogen, China. *Earth and Planetary Science Letters*, **161**, 215–230.

HACKER, B., WALLIS, S., RATSCHBACHER, L., GROVE, M. & GEHRELS, G. 2006. High-temperature geochronology constraints on the tectonic history and architecture of the ultrahigh-pressure Dabie-Sulu orogen. *Tectonics*, **25**, 1–17.

HARRIS, N. B. W., XU, R., LEWIS, C. L. & JIN, C. 1988. Plutonic rocks of the 1985 Tibet Geotraverse, Lhasa to Golmud. *Philosophical Transactions of the Royal Society of London, Series A*, **327**, 145–168.

HARROWFIELD, M. J. & WILSON, C. J. L. 2005. Indosinian deformation of the Songpan Garzê fold belt, northeast Tibetan plateau. *Journal of Structural Geology*, **27**, 101–117.

HSÜ, K. J., WANG, Q., LI, J., ZHOU, D. & SUN, S. 1987. Tectonic evolution of Qinling Mountains, China. *Eclogae Geologicae Helvetiae*, **80**, 735–752.

HUANG, M., MAAS, R., BUICK, I. S. & WILLIAMS, I. S. 2003. Crustal response to continental collisions between the Tibet, Indian, South China and North China blocks: geochronological constraints from the Songpan-Garzê orogenic belt, western China. *Journal of Metamorphic Geology*, **21**, 223–240.

HUANG, W. & WU, Z. W. 1992. Evolution of the Qin ling orogenic belt. *Tectonics*, **11**, 371–380.

JOLIVET, M., BRUNEL, M. *ET AL.* 2003. Neogene extension and volcanism in the Kunlun fault zone, northern Tibet: New constraints on the age of the Kunlun fault. *Tectonics*, **20**, 1052, doi: 10.1029/2002TC001428.

JOLIVET, M., BRUNEL, M. *ET AL.* 2001. Mesozoic and Cenozoic tectonics of the northern edge of the Tibetan Plateau; fission-track constraints. *Tectonophysics*, **343**, 111–134.

KAPP, P., YIN, A. *ET AL.* 2000. Blueschist-bearing metamorphic core complexes in the Qiangtang block reveal deep crustal structure of the northern Tibet. *Geology*, **28**, 19–22.

KIRBY, E., REINERS, P. W. *ET AL.* 2002. Late Cenozoic evolution of the eastern margin of the Tibetan plateau: Inferences from $^{40}Ar/^{39}Ar$ and (U–Th)/He thermochronology. *Tectonics*, **21**, doi: 10.1029/2000TC001246.

LAI, Q. Z., DING, L., WANG, H. W., YUE, Y. H. & CAI, F. L. 2007. Constraining the stepwise migration of the eastern Tibetan Plateau margin by apatite fission track thermochronology. *Science in China Series D: Earth Sciences*, **50**, 172–183.

LI, S., KUSKY, T. *ET AL.* 2007. Collision leading to multiple-stage extrusion in the Qinling orogen: insights from the Mianlue suture. *Gondwana Research*, **12**, 121–143.

MALAVIEILLE, J., MATTAUER, M., LANCELOT, J., CALASSOU, S., XU, Z. & HAO, Z. 1991. Large scale décollement in the Indosinian (Triassic) fold belt of Eastern Tibet. *Terra Abstracts*, **3**, 258.

MATTAUER, M., MALAVIEILLE, J. *ET AL.* 1992. La chaîne triasique de Songpan-Garzê (ouest Sechuan et Est Tibet); une chaîne de plissement-décollement sur marge passive. Translated title: The Songpan-Garzê Triassic belt of western Sichuan and eastern Tibet; a décollement-fold belt on a passive margin. *Comptes Rendus de l'Académie des Sciences Paris*, **314**, 619–626.

NIE, S., YIN, A., ROWLEY, D. B. & JIN, Y. 1994. Exhumation of the Dabie Shan ultra-high-pressure rocks and accumulation of the Songpan-Ganzi flysch sequence, central China. *Geology*, **22**, 999–1002.

PULLEN, A., KAPP, P., GEHRELS, G., VERVOOT, J. D. & DING, L. 2008. Triassic continental subduction in central Tibet and Mediterranean-style closure of the Paleo-Tethys Ocean. *Geology*, **36**, 351–354.

RATSCHBACHER, L., HACKER, B. R. *ET AL.* 2003. Tectonics of the Qinling (Central China): Tectonostratigraphy, geochronology and deformation history. *Tectonophysics*, **366**, 1–53, doi: 10.1016/S0040-1951(03)00053-2.

RAO, R. B., XU, J. F., CHEN, Y. & ZHOU, D. 1987. *The Triassic System of the Qinghai-Xizang Plateau*. Geological Publishing House, Beijing.

REID, A. J., FOWLER, A. P., PHILLIPS, D. & WILSON, C. J. L. 2005*a*. Thermochronology of the Yidun arc, central eastern Tibetan Plateau: constraints from $^{40}Ar/^{39}Ar$ K-feldspar and apatite fission track data. *Journal of Asian Earth Sciences*, **25**, 915–935.

REID, A. J., WILSON, C. J. L. & LIU, S. 2005*b*. Structural evidence for the Permo-Triassic tectonic evolution of the Yidun arc, eastern Tibetan plateau. *Journal of Structural Geology*, **27**, 119–137.

REID, A., WILSON, C. J. L., SHUN, L., PEARSON, N. & BELOUSOVA, E. 2007. Mesozoic plutons of the Yidun arc, SW China: U/Pb geochronology and Hf isotopic signature. *Ore Geology Reviews*, **34**, 88–106.

RICHARDSON, N. J., DENSMORE, A. L. *ET AL.* 2008. Extraordinary denudation in the Sichuan basin: Insights from low-temperature thermochronology adjacent to the eastern margin of the Tibetan Plateau. *Journal of Geophysical Research*, **113**, B044409, doi: 10.1029/2006JB004739.

ROBERT, A., ZHU, J. *ET AL.* 2010. Crustal structures in the area of the 2008 Sichuan Earthquake from geophysics and geology. *Tectonophysics*, **491**, 205–210.

ROGER, F., CALASSOU, S. *ET AL.* 1995. Miocene emplacement and deformation of the Konga Shan granite (Xianshui He fault, west Sichuan, China): Geodynamic implications. *Earth and Planetary Science Letters*, **130**, 201–216.

ROGER, F., ARNAUD, N. *ET AL.* 2003. Geochronological and geochemical constraints on Mesozoic suturing in East Central Tibet. *Tectonics*, **22**, 1037, doi: 10.1029/2002TC001466.

ROGER, F., MALAVIEILLE, J., LELOUP, P. H., CALASSOU, S. & XU, Z. 2004. Timing of granite emplacement and cooling in the Songpan-Garzê fold belt (eastern Tibetan Plateau) with tectonic implications. *Journal of Asian Earth Sciences*, **22**, 465–481.

ROGER, F., JOLIVET, M. & MALAVIEILLE, J. 2008. Tectonic Evolution of the Triassic Fold Belts of Tibet. *Comptes Rendus Geoscience, Académie des Sciences*, Paris, **340**, 180–189.

ROGER, F., JOLIVET, M. & MALAVIEILLE, J. 2010. The tectonic evolution of the Songpan Garzê (North Tibet). *Journal of Asian Earth Sciences*, **39**, 254–269.

ROWLEY, D. B., XUE, F., TUCKER, R. D., PENG, Z. X., BAKER, J. & DAVIS, A. 1997. Ages of ultrahigh pressure metamorphism and protolith orthogneisses from the eastern Dabie Shan: U/Pb zircon geochronology. *Earth and Planetary Science Letters*, **151**, 191–203.

SENGÖR, A. M. C. 1985. East Asian tectonics collage. *Nature*, **318**, 15–17.

TURCOTTE, D. L. & SCHUBERT, G. 2002. *Geodynamics.* Cambridge University Press, Cambridge.

VINCENT, S. J. & ALLEN, M. B. 1999. Evolution of the Mule and Chaoshui basins, China; implications for Mesozoic strike–slip basin formation in Central Asia. *Geological Society of America Bulletin*, **111**, 725–742.

WALLIS, S., TSUJIMORI, T., AOYA, M., KAWAKAMI, T., TERADA, K., SUZUKI, K. & HYODO, H. 2003. Cenozoic and Mesozoic metamorphism in the Longmenshan orogen: Implications for geodynamic models of eastern Tibet. *Geology*, **31**, 745–748.

Wang, C. Y., Han, W. B. *et al.* 2007. Crustal structure beneath the eastern margin of the Tibetan Plateau and its tectonic implications. *Journal of Geophysical Research*, **112**, B07307; doi: 10.1029/2005JB003873.

Wilson, C. J. L., Harrowfield, M. J. & Reid, A. J. 2006. Brittle modification of Triassic architecture in eastern Tibet: implications for the construction of the Cenozoic plateau. *Journal of Asian Earth Sciences*, **27**, 341–357.

Xiao, L. & Clemens, J. D. 2007. Origin of potassic (C-type) adakite magmas: experimental and field constraints. *Lithos*, **95**, 399–414.

Xiao, L., Zhang, H. F. *et al.* 2007. Late Triassic granitoids of the eastern margin of the Tibetan Plateau: Geochronology, petrogenesis and implications for tectonic evolution. *Lithos*, **96**, 436–452.

Xu, G. & Kamp, P. J. J. 2000. Tectonics and denudation adjacent to the Xianshuihe Fault, eastern Tibetan Plateau: Constraints from fission track thermochronology. *Journal of Geophysical Research*, **105**, 19 231–19 251.

Xu, Z. Q., Hou, L. & Wang, Z. 1992. *Orogenic Processes of the Songpan-Garzê Orogenic Belt of China*. Geological Publishing House, Beijing.

Xu, L., Rondenay, S. & Van Der Hilst, R. D. 2007. Structure of the crust beneath the southeastern Tibetan Plateau from teleseismic receiver functions. *Physics of the Earth and Planetary Interiors*, **165**, 176–193.

Zhang, C. Z., Li, B., Cai, J. X., Tang, X. C., Wei, Q. G. & Zhang, Y. X. 2008*a*. A-type granite and adakitic magmatism association in Songpan-Garze fold belt, eastern Tibetan Plateau: Implication for lithospheric delamination: comment. *Lithos*, **103**, 562–564.

Zhang, H., Zhang, B., Harris, N., Zhang, L., Chen, Y., Chen, N. & Zhao, Z. 2006. U–Pb zircon SHRIMP ages, geochemical and Sr–Nd–Pb isotopic compositions of intrusive rocks from the Longshan-Tianshui area in the southeast corner of the Qilian orogenic belt, China: Constraints on petrogenesis and tectonic affinity. *Journal of Asian Earth Sciences*, **27**, 751–764.

Zhang, H. F., Parrish, R., Zhang, L., Xu, W. C., Yuan, H. L., Gao, S. & Crowley, Q. G 2007. A-type granite and adakitic magmatism association in Songpan-Garze fold belt, eastern Tibetan Plateau: Implication for lithospheric delamination. *Lithos*, **97**, 323–335; doi: 10.1016/j.lithos.2007.01.002.

Zhang, H. F., Parrish, R., Zhang, L., Xu, W. C., Yuan, H. L., Gao, S. & Crowley, Q. G. 2008*b*. Reply to the comment by Zhang *et al.* on: 'First finding of A-type and adakitic magmatism association in Songpan-Garze fold belt, eastern Tibetan Plateau: implication for lithospheric delamination. *Lithos*, **103**, 565–568.

Zheng, D., Zhang, P-Z. *et al.* 2006. Rapid exhumation at ~8 Ma on the Liupan Shan thrust fault from apatite fission-track thermochronology: Implications for growth of the northeastern Tibetan Plateau margin. *Earth and Planetary Science Letters*, **248**, 198–208.

Zhou, M. F., Yan, D. P., Vasconcelos, P. M., Li, J. W. & Hu, R. Z. 2008. Structural and geochronological constraints on the tectono-thermal evolution of the Danba domal terrane, eastern margin of the Tibetan plateau. *Journal of Asian Earth Sciences*, **33**, 414–427.

Zi, J., Fan, W., Wang, Y., Peng, T. & Guo, F. 2008. Geochemistry and petrogenesis of the Permian mafic dykes in the Panxi region, SW China. *Gondwana Research*, **14**, 368–382.

Zou, D. B., Chen, L. K., Rao, R. B. & Chen, Y. M. 1984. On the Triassic turbidite in the southern Bayan-Har mountain region. *Contribution to the Geology of the Qinghai-Xizang (Tibet) Plateau*, **15**, 27–39.